

Observational constraints on one-parameter dynamical dark-energy parametrizations and the H_0 tension

Weiqliang Yang,^{1,*} Supriya Pan,^{2,†} Eleonora Di Valentino,^{3,‡}
Emmanuel N. Saridakis,^{4,5,§} and Subenoy Chakraborty^{6,¶}

¹*Department of Physics, Liaoning Normal University, Dalian, 116029, P. R. China*

²*Department of Mathematics, Presidency University, 86/1 College Street, Kolkata 700073, India*

³*Jodrell Bank Center for Astrophysics, School of Physics and Astronomy,*

University of Manchester, Oxford Road, Manchester, M13 9PL, UK

⁴*Physics Division, National Technical University of Athens, 15780 Zografou Campus, Athens, Greece*

⁵*CASPER, Physics Department, Baylor University, Waco, TX 76798-7310, USA*

⁶*Department of Mathematics, Jadavpur University, Kolkata 700032, West Bengal, India*

The phenomenological parametrizations of dark-energy (DE) equation of state can be very helpful, since they allow for the investigation of its cosmological behavior despite the fact that its underlying theory is unknown. However, although there has been a large amount of research on DE parametrizations which involve two or more free parameters, the one-parameter parametrizations seem to be underestimated. We perform a detailed observational confrontation of five one-parameter DE models, with observational data from cosmic microwave background (CMB), Joint light-curve analysis sample from Supernovae Type Ia observations (JLA), baryon acoustic oscillations (BAO) distance measurements, and cosmic chronometers (CC). We find that all models favor a phantom DE equation of state at present time, while they lead to H_0 values in perfect agreement with its direct measurements and therefore they offer an alleviation to the H_0 -tension. Finally, performing a Bayesian analysis we show that although Λ CDM cosmology is still favored, one-parameter DE models have similar or better efficiency in fitting the data comparing to two-parameter DE parametrizations, and thus they deserve a thorough investigation.

PACS numbers: 98.80.-k, 95.36.+x, 98.80.Es

I. INTRODUCTION

The remarkable journey of modern cosmology started in 1998, when the observational evidences showed that we are living in an accelerating universe and that the previous physical scenarios needed to be retraced. The introduction of dark energy (DE) concept was a need in order for the observational predictions to acquire a solid theoretical formulation. The dark energy is a component with high negative pressure that drives the universe acceleration, nevertheless its nature has remained a mysterious chapter in the scientific history after a series of investigations by a large number of researchers. The cosmological constant is the simplest DE fluid with the above features, however the “cosmological constant problem” [1] and the possibility that the DE sector could be dynamical led to a number of explanations, mainly in two directions. The first is to consider that the DE sector corresponds to a peculiar extra fluid that fills the universe in the framework of general relativity [2, 3]. The second direction is to consider that the DE fluid is an effective one, arising from a modification of the gravitational sector itself [4, 5, 6].

Independently of the underlying nature and the micro-physical theory of DE, one can introduce phenomenological parametrizations of the DE equation-of-state parameter $w_x = p_x/\rho_x$, where p_x and ρ_x are respectively the pressure and energy density of the (effective) DE perfect fluid, which is considered to have a dynamical character in general. Since for the moment we do not have any fundamental rule in favor of some specific equation-of-state parameters, we may consider various functional forms for w_x . For a literature survey of various DE parametrizations and models we refer to the works [7, 8, 9, 10, 11, 12, 13, 14, 15, 16, 17, 18, 19, 20, 21, 22, 23, 24, 25, 26, 27, 28, 29, 30, 31, 32, 33, 34, 35, 36, 37, 38, 39, 40, 41, 42, 43, 44].

In general, the well known DE parametrizations have two free parameters, usually denoted by w_0w_a CDM models, where w_0 marks the present value of w_x and w_a characterizes the dynamical nature of the DE sector. However, apart

*Electronic address: d11102004@163.com

†Electronic address: supriya.maths@presiuniv.ac.in

‡Electronic address: eleonora.divalentino@manchester.ac.uk

§Electronic address: Emmanuel_Saridakis@baylor.edu

¶Electronic address: schakraborty@math.jdvu.ac.in

from the w_0w_a CDM parametrizations, one-parameter dynamical DE parametrizations, as well as models with more than two parameters, have also been introduced and investigated in the last years. Nevertheless, the one-parameter dynamical DE parametrizations are much neglected in the literature compared to the DE parametrizations having two or more parameters. In principle we do not find any strong reason behind this underestimation, and thus in this work we aim to investigate the features of this particular class of DE parametrizations, and explore its cosmological viabilities with the recent observational evidences, taking into account their advantage that they are more economical and have less number of free parameters compared to other dark energy models with two or more than two free parameters.

Hence, we introduce various one-parameter dynamical DE parametrizations that are primarily motivated from the phenomenological ground, and we perform a detailed observational confrontation. In particular, we use data from cosmic microwave background (CMB) observations, from Joint light-curve analysis sample from Supernovae Type Ia observations (JLA), from baryon acoustic oscillations (BAO) distance measurements, as well as from cosmic chronometers Hubble parameter measurements (CC), performing additionally various combined analyses.

The manuscript is organized as follows. In Section II we present the basic equations for a general dark-energy scenario at both the background and perturbation level, and we display the five one-parameter DE parametrizations that are going to be investigated. In Section III we describe the observational data sets that will be used. In Section IV we perform the observational confrontation, extracting the observational constraints on the various cosmological quantities. After that in Section V we compare the present dynamical DE parametrizations mainly through the Bayesian analysis. Finally, we close the present work in Section VI with a brief summary.

II. ONE-PARAMETER PARAMETRIZATIONS AT BACKGROUND AND PERTURBATION LEVELS

In this section we present the basic equations that determine the universe evolution at both the background and perturbation levels, and we introduce various one-parameter parametrizations for the dark-energy equation-of-state parameter. Throughout the work we consider the homogeneous and isotropic Friedmann-Lemaître-Robertson-Walker (FLRW) geometry, with metric

$$ds^2 = -dt^2 + a^2(t) \left[\frac{dr^2}{1 - Kr^2} + r^2 (d\theta^2 + \sin^2\theta d\phi^2) \right], \quad (1)$$

where $a(t)$ is the scale factor and K determines the spatial curvature, with values 0, -1 and $+1$ corresponding to spatially flat, open and closed universe, respectively.

We consider a universe filled with radiation, baryons and cold dark matter, and we additionally consider the DE fluid. In this case the Friedmann equations, that determine the universe evolution at the background level, read as

$$H^2 + \frac{K}{a^2} = \frac{8\pi G}{3} \rho_{tot}, \quad (2)$$

$$2\dot{H} + 3H^2 + \frac{K}{a^2} = -8\pi G p_{tot}, \quad (3)$$

with G the Newton's constant and $H = \dot{a}/a$ the Hubble function of the FLRW universe, with dots denoting derivatives with respect to cosmic time. In the above expressions we have introduced the total energy density and pressure as $\rho_{tot} = \rho_r + \rho_b + \rho_c + \rho_x$ and $p_{tot} = p_r + p_b + p_c + p_x$ respectively, with the symbols r , b , c , x denoting radiation, baryon, cold dark matter and dark energy fluids. Finally, for simplicity in the following we will focus on the spatially flat case ($K = 0$) since it is favored by observations.

As usual we assume that the above sectors do not have any mutual interaction, and thus the conservation equation of each fluid is

$$\dot{\rho}_i + 3H(1 + w_i)\rho_i = 0, \quad (4)$$

where $i \in \{r, b, c, x\}$ and $p_i = w_i\rho_i$, w_i being the barotropic state parameter for the i -th fluid. Note that out of equations (2), (3) and (4), only two are independent. Hence, using the known equation-of-state parameters $w_r = 1/3$, $w_b = w_c = 0$, in (4) one can explicitly write down the conservation equations for radiation, baryons and cold dark matter respectively as, $\rho_r = \rho_{r0} a^{-4}$, $\rho_b = \rho_{b0} a^{-3}$ and $\rho_c = \rho_{c0} a^{-3}$, with ρ_{i0} the present value of ρ_i and where we have set the present scale factor a_0 to 1. Similarly, concerning the dark energy sector, equation (4) leads to

$$\rho_x = \rho_{x,0} \left(\frac{a}{a_0} \right)^{-3} \exp \left[-3 \int_{a_0}^a \frac{w_x(a')}{a'} da' \right]. \quad (5)$$

Thus, the evolution equation (5) implies that the dynamics of DE can be determined as long as a specific parametrization of the DE equation of state is given.

Having presented the equations that determine the universe evolution at the background level, we now proceed to the investigation of its evolution at the perturbation level, since this is related to the observed structure formation. In order to study the perturbation equations, one needs to consider the perturbed FLRW metric either in synchronous or in conformal Newtonian gauge. In the following we consider the former choice, in which the perturbed metric takes the form

$$ds^2 = a^2(\eta) [-d\eta^2 + (\delta_{ij} + h_{ij})dx^i dx^j], \quad (6)$$

where η is the conformal time, and δ_{ij} , h_{ij} are respectively the unperturbed and the perturbed metric tensors. Now, in the synchronous gauge the conservation equations of energy and momentum for the i -th component of the fluid for a mode with wavenumber k can be written as [45, 46, 47]:

$$\delta'_i = -(1 + w_i) \left(\theta_i + \frac{h'}{2} \right) - 3\mathcal{H} \left(\frac{\delta p_i}{\delta \rho_i} - w_i \right) \delta_i - 9\mathcal{H}^2 \left(\frac{\delta p_i}{\delta \rho_i} - c_{a,i}^2 \right) (1 + w_i) \frac{\theta_i}{k^2}, \quad (7)$$

$$\theta'_i = -\mathcal{H} \left(1 - 3 \frac{\delta p_i}{\delta \rho_i} \right) \theta_i + \frac{\delta p_i / \delta \rho_i}{1 + w_i} k^2 \delta_i - k^2 \sigma_i, \quad (8)$$

where primes mark derivatives with respect to conformal time and $\mathcal{H} = a'/a$ is the conformal Hubble parameter. Furthermore, $\delta_i = \delta \rho_i / \rho_i$ is the density perturbation for the i -th fluid, $\theta_i \equiv ik^j v_j$ denotes the divergence of the i -th fluid velocity, $h = h_j^j$ stands for the trace of the metric perturbations h_{ij} , and σ_i is the anisotropic stress related to the i -th fluid. Finally, the quantity $c_{a,i}^2 = \dot{p}_i / \dot{\rho}_i$ denotes the adiabatic speed of sound of the i -th fluid, and it is given by $c_{a,i}^2 = w_i - \frac{w'_i}{3\mathcal{H}(1+w_i)}$ in the case where we set the sound speed $c_s^2 = \delta p_i / \delta \rho_i$ to 1. In the following analysis we neglect the anisotropic stress for simplicity.

In this work we are interested in investigating one-parameter DE equation-of-state parametrizations. In particular, we consider five such parametrizations given by:

$$\text{Model I: } w_x(a) = w_0 \exp(a - 1), \quad (9)$$

$$\text{Model II: } w_x(a) = w_0 a [1 - \log(a)], \quad (10)$$

$$\text{Model III: } w_x(a) = w_0 a \exp(1 - a), \quad (11)$$

$$\text{Model IV: } w_x(a) = w_0 a [1 + \sin(1 - a)], \quad (12)$$

$$\text{Model V: } w_x(a) = w_0 a [1 + \arcsin(1 - a)], \quad (13)$$

where w_0 is the only free parameter, corresponding to the dark energy equation-of-state parameter at present. In order to provide a more transparent picture of the behavior of the above parametrizations, in Fig. 1 we depict $w_x(a)$, taking two cases for w_0 , namely one lying in the quintessence and one lying in the phantom regime. As we can see, in all models $w_x(a)$ presents a decreasing behavior.

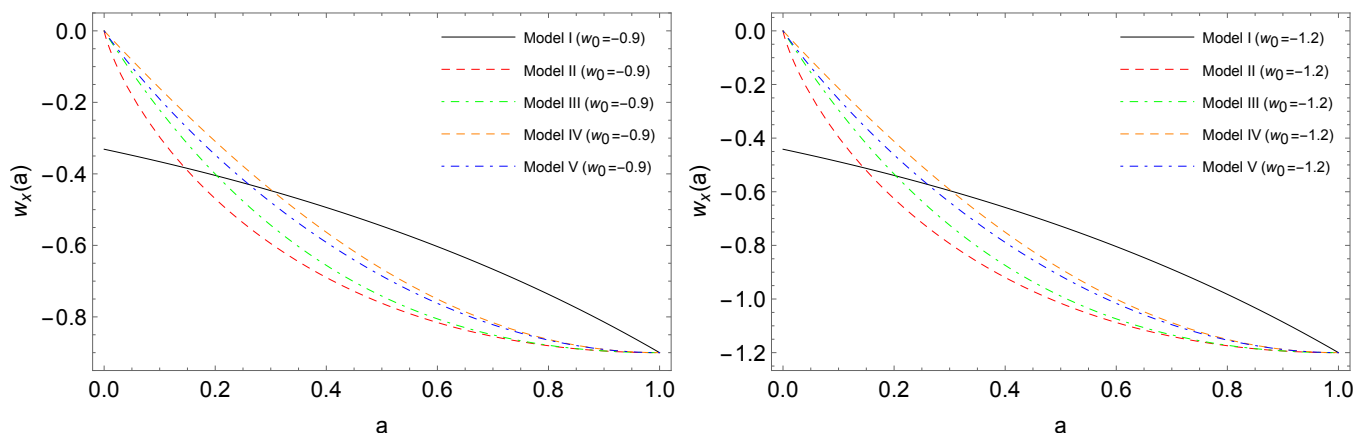


FIG. 1: The evolution of the one-parameter dynamical DE equation-of-state parametrizations (9)-(13) as a function of the scale factor, for $w_0 = -0.9$ (left graph) and $w_0 = -1.2$ (right graph).

III. OBSERVATIONAL DATA

In this section we proceed to a detailed observational confrontation of the one-parameter dynamical DE equation-of-state parametrizations (9)-(13) presented in the previous section. We analyze several combinations of cosmological data, by considering the six cosmological parameters of the standard Λ CDM paradigm: the baryon and the cold dark matter energy densities $\Omega_b h^2$ and $\Omega_c h^2$, the ratio between the sound horizon and the angular diameter distance at decoupling Θ_s , the reionization optical depth τ , and the spectral index and the amplitude of the scalar primordial power spectrum n_s and A_s . Moreover, for the various models we add the free parameter w_0 , which parametrizes the DE evolution. All these 7 free parameters are explored within the range of the conservative flat priors listed in Table I.

Parameter	prior
$\Omega_b h^2$	[0.013, 0.033]
$\Omega_c h^2$	[0.001, 0.99]
Θ_s	[0.5, 10]
τ	[0.01, 0.8]
n_s	[0.7, 1.3]
$\log A$	[1.7, 5.0]
w_0	[-2, 0]

TABLE I: Summary of the flat priors on the cosmological parameters assumed in this work, for the different DE parametrizations (9)-(13).

We derive the bounds on the cosmological parameters by analyzing the full range of the 2015 Planck temperature and polarization cosmic microwave background (CMB) angular power spectra, and we call this combination ‘‘CMB’’ [48, 49]. Additionally, we consider the Joint light-curve analysis sample from Supernovae Type Ia and we refer to this dataset as ‘‘JLA’’ [50]. Furthermore, we add the baryon acoustic oscillations (BAO) distance measurements, and we call them ‘‘BAO’’ [51, 52, 53]. Finally, we use the Hubble parameter measurements from the cosmic chronometers (CC) and we refer to them as ‘‘CC’’ [54].

In order to analyze statistically the several combinations of datasets, exploring the different dynamical DE scenarios, we use our modified version of the publicly available Monte-Carlo Markov Chain package *Cosmomc* [55], including the support for the Planck data release 2015 Likelihood Code [49]¹. This has a convergence diagnostic based on the Gelman and Rubin statistic and implements an efficient sampling of the posterior distribution using the fast/slow parameter de-correlations [56].

IV. RESULTS

In this section we present the observational constraints and their implications for all the one-parameter DE parametrizations (9)-(13). All models are confronted initially with CMB data alone, and then with different combinations of cosmological data. In the Appendix we show all Tables containing the constraints on the model parameters for all observational datasets used in this work. Additionally, in Fig. 2 we concisely display the constraints on the present value of the dark energy equation of state w_0 , for all models, considering all observational datasets. In the following we investigate the one parameter DE models in detail, presenting their observational consequences.

We start by investigating Model I of (9), namely $w_x(a) = w_0 \exp(a - 1)$. In Fig. 3 we can see the effects of different w_0 values on the temperature and matter power spectra. The results of the observational analysis of this model can be seen in Table IV of the Appendix, where we display the 68% and 95% confidence level (CL) constraints for various quantities while the full contour plots are presented in Fig. 4.

As we observe from Table IV (see Appendix), the CMB data alone allow a very large value of the Hubble constant at present and moreover its error bars are significantly large: $H_0 = 74^{+11}_{-7}$ at 68% CL ($H_0 = 74^{+14}_{-15}$ at 95% CL). The constraint on H_0 is actually very close to its local measurements [57], recently confirmed by [58] and [59].

¹ See <http://cosmologist.info/cosmomc/>

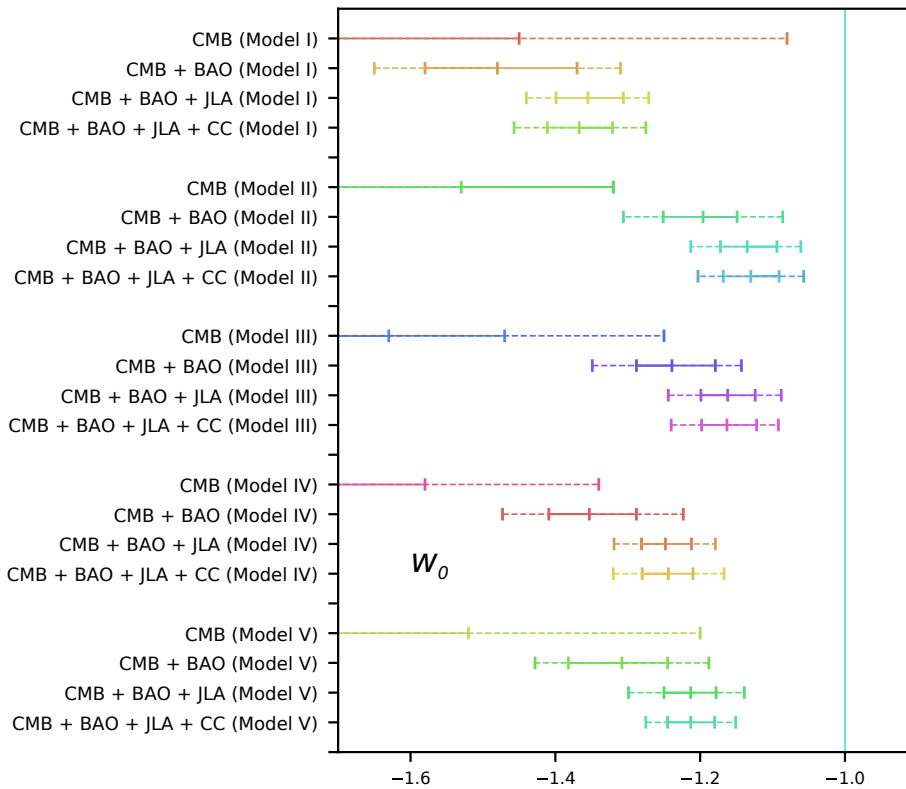


FIG. 2: Whisker graph with the 68% CL (solid line) and 95% CL (dashed line) regions for the free model parameter w_0 of the DE parametrizations (9)-(13), for the combination of datasets considered in this work.

From the Table IV we see that the present value of the DE equation-of-state parameter for CMB alone is found to prefer a phantom dark energy scenario, namely $w_0 < -1$, at more than 95% CL. Consequently, the matter density parameter decreases and acquires a very low value ($\Omega_{m0} = 0.268^{+0.038}_{-0.081}$ at 68% CL). However, since these Ω_{m0} and σ_8 are anti-correlated, while σ_8 is positively correlated with H_0 (see Fig. 4), hence, this does not correspond to the alleviation of the $S_8 = \sigma_8 \sqrt{\Omega_{m0}/0.3}$ tension of Planck's indirect estimation with its direct measurements from cosmic shear experiments like the Canada France Hawaii Lensing Survey (CFHTLenS) [60, 61], the Kilo Degree Survey of 450 deg² of imaging data (KiDS-450) [62], and the Dark Energy Survey (DES) [63].

When the BAO data are added to CMB, the constraints on the model parameters are significantly improved and the error bars on most of the parameters, in particular w_0 , Ω_{m0} , σ_8 and H_0 , are decreased. The mean value of the Hubble constant slightly shifts towards a lower value, and the DE equation of state at present, w_0 , moves towards a smaller one ($w_0 = -1.48 \pm 0.10$ at 68% CL) comparing to its estimation from CMB alone ($w_0 < -1.45$ at 68% CL). As one can see, the CMB+BAO data also assure the validity of $w_0 < -1$ at more than 99% CL. The interesting output of this analysis is that the constraint on H_0 is again found to be very close to its estimation by local measurements [57].

The addition of JLA to the former data set combination (i.e., CMB+BAO) further improves the cosmological constraints, as one can clearly see from Table IV (see Appendix). In particular, we see that H_0 again shifts down and w_0 up, with decreasing error bars. An analogous improvement of the bounds can be seen for Ω_{m0} and σ_8 . Although the estimation of H_0 from this analysis decreases in comparison to the previous results of CMB and CMB+BAO, within 95% CL, it can still match the direct estimation [57]. Furthermore, the DE equation of state at present is again found to be in phantom regime.

We close the analysis by adding the CC dataset, nevertheless the results for the data combination CMB+BAO+JLA+CC do not exhibit significant differences from the previous case CMB+BAO+JLA.

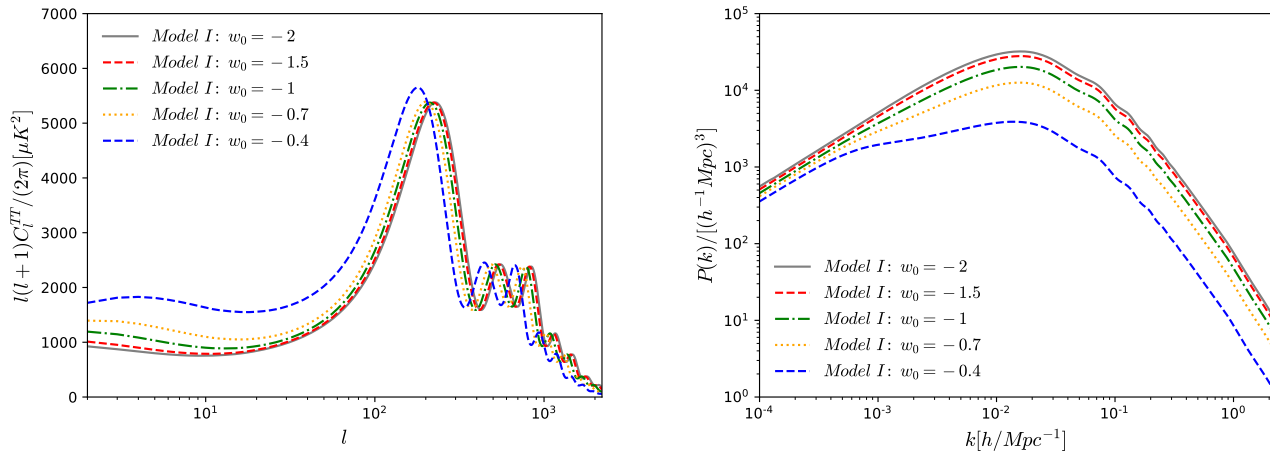


FIG. 3: The CMB TT spectra (left graph) and the matter power spectra (right graph), for Model I of (9), namely $w_x(a) = w_0 \exp(a - 1)$, for various values of the free model parameter w_0 .

In summary, the observational analysis for Model I shows that $w_0 < -1$ at more than 95% CL for CMB only, while the tension on H_0 seems to be alleviated. The addition of JLA shifts H_0 towards lower values, but still in agreement within 2σ with [57], while the addition of CC does not affect the results significantly. The contour plot in the $w_0 - H_0$ plane can be seen in lower left graph of Fig. 4. The preference for a phantom DE equation of state is due to the better fit of the large scales of the temperature power spectrum, that prefers a lower quadrupole with respect to the Λ CDM scenario, as can be clearly seen in Fig. 5.

Finally, comparing the results obtained for Model I with the constraints released by the Planck collaboration [64] for the w CDM or $w_0 w_a$ CDM models, we can notice that for Model I using only CMB data the H_0 value is well constrained by the data and is close to its directly measured value [57], while it has a slightly lower limit for the Planck's extended scenario (that means the $w_0 w_a$ CDM scenario). On the other hand, when adding the BAO data, the H_0 value is still high and in agreement with [57], while in the Planck case the Hubble constant decreases leading to the aforementioned tension. In this context we refer to a recent work [65] discussing the tensions in the cosmological parameters from various observational data and some possible explanations.

We now investigate Model II of (10), namely $w_x(a) = w_0 a [1 - \log(a)]$. In Table V of the Appendix we summarize the observational constraints arising from various data combinations. We do not explicitly present the corresponding contour plots since they are similar to the ones of Model I.

Comparing the results with those of Model I above, we can see that for Model II considering the CMB data alone, H_0 acquires higher values ($H_0 = 81_{-9}^{+12}$ at 68% CL) and w_0 indicates a strong evidence for a phantom equation of state which remains at more than 95% CL. Moreover, similarly to Model I, for Model II we also observe that the combinations CMB+BAO, CMB+BAO+JLA and CMB+BAO+JLA+CC significantly improve the constraints and reduce the error bars on the parameters. In particular, the H_0 mean value shifts towards lower values and we find $w_0 < -1$ at more than 95% CL for all data combinations. Note that from Table V (see Appendix) we see that for the data set CMB+BAO the estimated value of H_0 is in agreement within 1 standard deviation with the local estimation of [57] and thus the H_0 -tension is alleviated (H_0 is higher than the one estimated by Planck 2015 [66] for the base Λ CDM scenario, and it is in perfect agreement to [57]). Additionally, for the last two combinations CMB+BAO+JLA and CMB+BAO+JLA+CC we observe that while the Hubble constant is always in agreement within 2σ with [57], in contrast to Model I w_0 prefers a lower phantom mean value, but still with high significance. Finally, similar to the previous model, the σ_8 tension is not reconciled.

We proceed to the investigation of Model III of (11), namely $w_x(a) = w_0 a \exp(1 - a)$. Using the same observational datasets, in Table VI of the Appendix we summarize the observational constraints on this model.

As we can see, for the CMB data alone the Hubble parameter acquires an even larger mean value in comparison to the previous models, while the DE equation-of-state parameter at present obtains a smaller value, namely $w_0 = -1.63_{-0.37}^{+0.38}$ at 95% CL. Similarly to the previous model, we find that the inclusion of any external data set, namely BAO, JLA or CC, to CMB significantly improves the constraints, and $w_0 < -1$ is still valid up to 95% CL. For the combination of CMB+BAO data we see that the estimated value of $H_0 = 71.4_{-1.6}^{+1.4}$ (at 68%

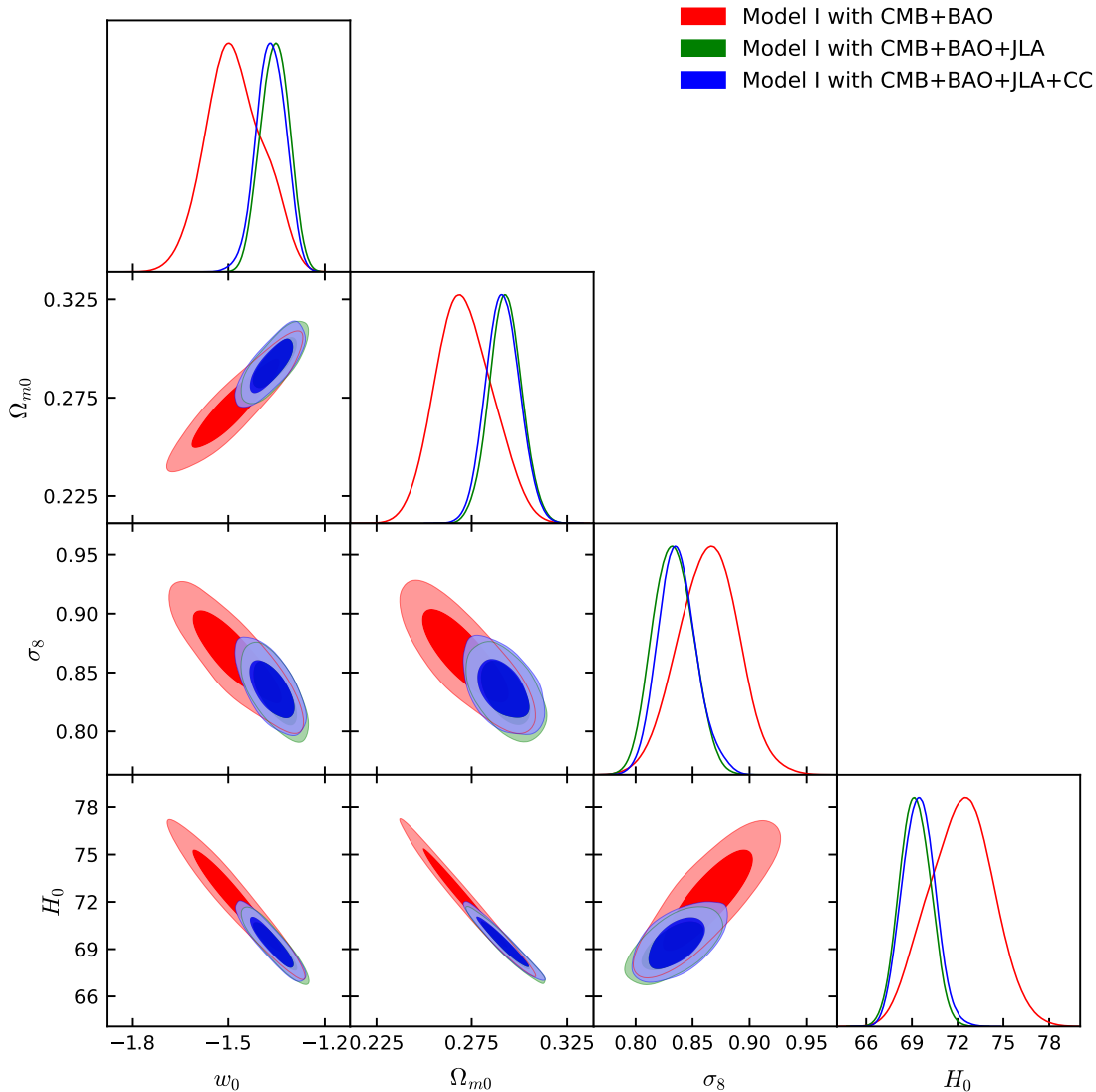


FIG. 4: The 2D contour plots for several combinations of various quantities for Model I of (9), namely $w_x(a) = w_0 \exp(a - 1)$, and the corresponding 1D posterior distributions.

CL) is perfectly in agreement to its local estimation of [57], alleviating the H_0 -tension. Moreover, concerning w_0 we can note that it is constrained to be $w_0 = -1.239^{+0.060}_{-0.049}$ (at 68% CL) which is phantom at more than 3σ . The addition of JLA to CMB+BAO decreases the error bars on H_0 , Ω_{m0} and σ_8 , while within 95% CL this model seems to alleviate the tension on H_0 . Finally, the combination CMB+BAO+JLA+CC does not offer any notable differences compared to the analysis with CMB+BAO+JLA, and thus similar conclusions are achieved.

We investigate Model IV of (12), namely $w_x(a) = w_0 a [1 + \sin(1 - a)]$. In Table VII of the Appendix we summarize the observational constraints arising from various data combinations.

As we see, the estimations of the Hubble parameter for all the dataset combinations are shifted towards higher values than Λ CDM. For the CMB data only, H_0 acquires values comparable with Model III, i.e. $H_0 = 84.3^{+9.9}_{-6.5}$ at 68% CL. As before, the inclusion of any external data set significantly improves the constraints on the cosmological parameters, decreasing the error bars. A common feature for all the analyses is that w_0 remains in the phantom regime at more than 95% CL. Furthermore, for this model the CMB+BAO+JLA and CMB+BAO+JLA+CC data combinations favor a phantom DE equation of state at many standard deviations. Additionally, it is clearly seen that the H_0 -tension is alleviated for all the combinations considered, apart from the CMB data alone which predict a quite high H_0 value.

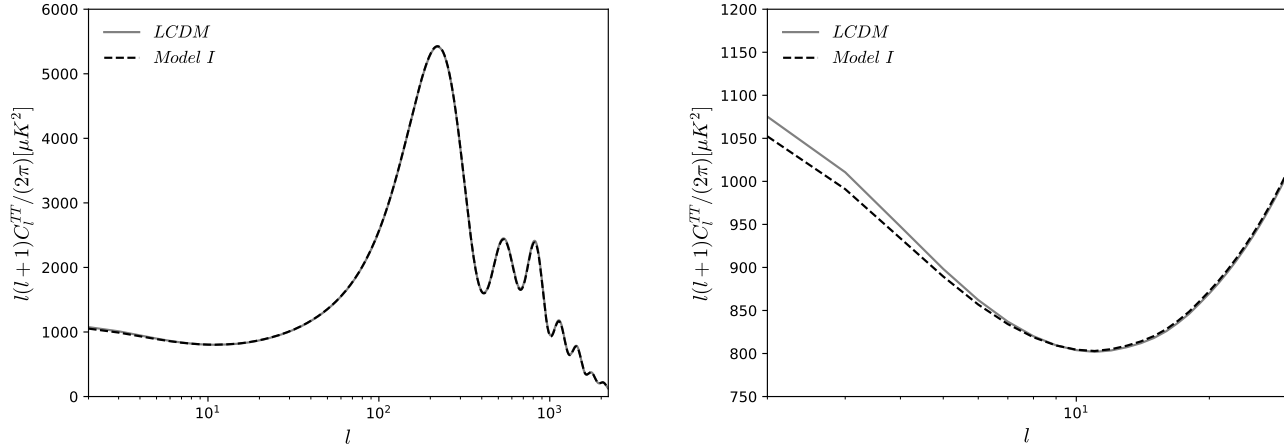


FIG. 5: Comparison between the best fit for the Λ CDM paradigm and for the Model I of (9), namely $w_x(a) = w_0 \exp(a - 1)$. While the curves are almost indistinguishable in the high multipole range, at large scales Model I can better recover the lower quadrupole of the data.

We close our analysis with the investigation of Model V of (13), namely $w_x(a) = w_0 a [1 + \arcsin(1 - a)]$. In a similar fashion, using the same observational datasets, in Table VIII of the Appendix we summarize the observational constraints on this model.

As we observe, we can clearly notice that this model maintains a similar trend compared to the previous four dynamical DE models. The present value of the DE equation-of-state parameter is constrained in the phantom regime up to 99% CL. The Hubble parameter acquires a very large value for the CMB data only ($H_0 = 82.9^{+12}_{-7.0}$ at 68% CL) with large error bars, however for the other data combinations H_0 and its errors bars decrease, and it becomes clear that the H_0 -tension can be alleviated.

V. MODEL COMPARISON AND THE BAYESIAN EVIDENCE

In the previous section we present the observational analysis and we extracted the constraints on various cosmological parameters of the five examined models. Concerning the dark energy equation of state at present, w_0 , we have already presented its constraints at 68% and 95% CL through the Whisker graph in Fig. 2 for all the one parameter DE models as well as considering all the observational datasets employed in this work. As we mentioned above, we observe that in all models a phantom DE equation-of-state parameter at current time is favored. Moreover, from Fig. 2 we may also note that the extracted w_0 for Model II and III using the common datasets, namely, CMB+BAO, CMB+BAO+JLA and CMB+BAO+JLA+CC, are relatively close to the cosmological constant boundary $w_0 = -1$, compared to other three models. Additionally, in order to present in a more transparent way the alleviation of the H_0 -tension, in Fig. 6 we summarize the contour plots in the $w_0 - H_0$ plane for all the examined models. From the figure one can notice that the parameters H_0 and w_0 are correlated to each other.

The question that arises naturally is which of the five models exhibits a better behavior, and moreover how efficient are they comparing to standard Λ CDM cosmology. Hence, we close our work with examining the Bayesian evidence of each of the five models analyzed above, compared to the reference Λ CDM cosmological scenario. The Bayesian evidence plays a crucial role in determining the observational support of any cosmological model. The involved calculation is performed through the publicly available code `MCEvidence` [67, 68]². We mention that `MCEvidence` needs only the MCMC chains that are used to extract the parameters of the models.

In Bayesian analysis one needs to evaluate the posterior probability of the model parameters θ , given a particular

² See github.com/yabebalFantaye/MCEvidence.

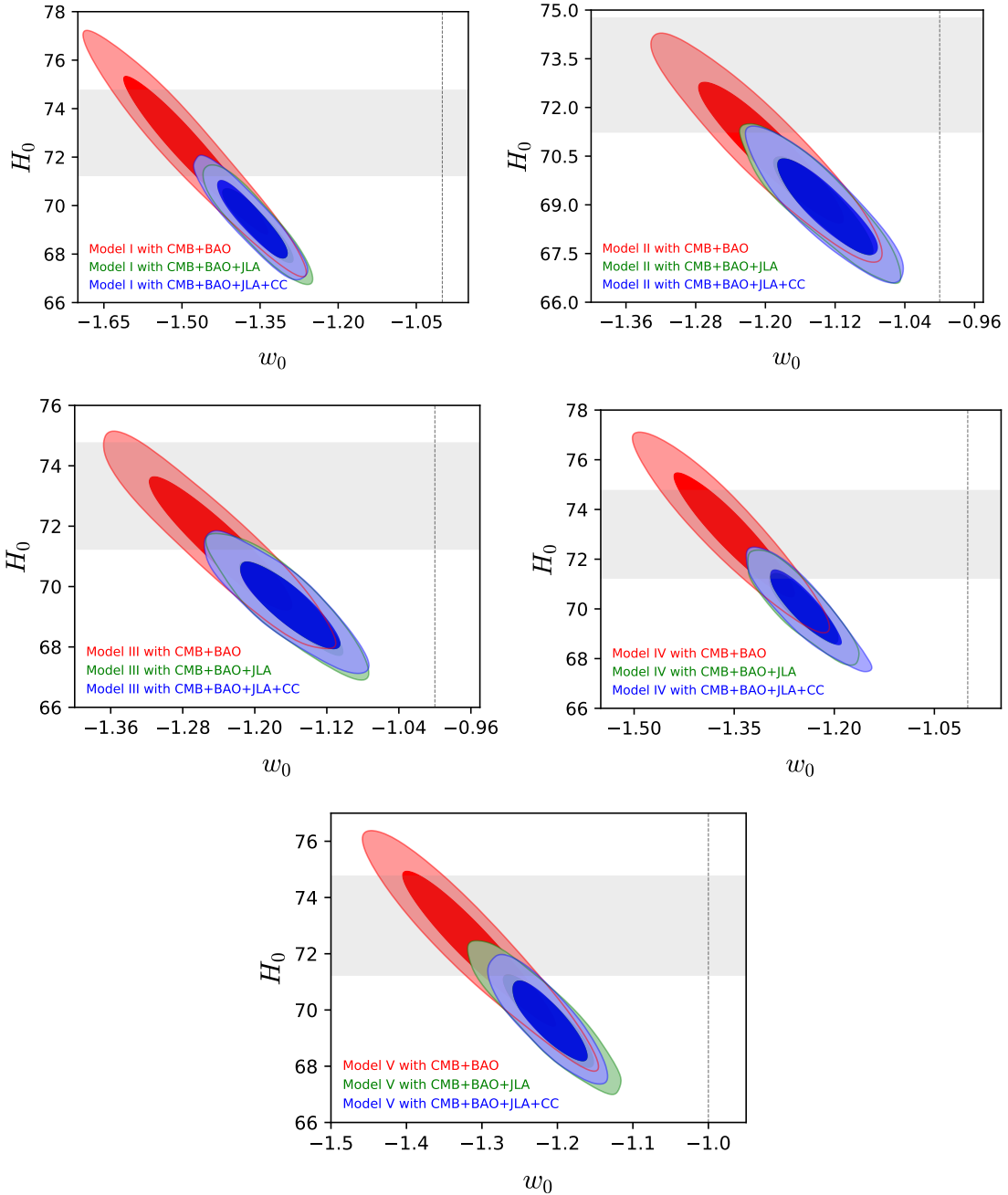


FIG. 6: Contour plots at the 68% and 95% CL on the $w_0 - H_0$ plane for the five models of one-parameter DE parametrizations (9)-(13), for various combinations of datasets. The gray horizontal band is the 68% CL Hubble parameter value corresponding to the direct measurement of [57], while the dotted vertical line marks the cosmological constant value $w_0 = -1$.

observational dataset x with any prior information for a model M . Using the Bayes theorem one can write

$$p(\theta|x, M) = \frac{p(x|\theta, M) \pi(\theta|M)}{p(x|M)}, \quad (14)$$

where the quantity $p(x|\theta, M)$ refers to the likelihood as a function of θ with $\pi(\theta|M)$ the prior information. The quantity $p(x|M)$ that appears in the denominator of (14) is known as the Bayesian evidence used for the model comparison. Let us note that this Bayesian evidence is the integral over the non-normalized posterior $\tilde{p}(\theta|x, M) \equiv p(x|\theta, M) \pi(\theta|M)$,

given by

$$E \equiv p(x|M) = \int d\theta p(x|\theta, M) \pi(\theta|M). \quad (15)$$

Now, for any cosmological model M_i and the reference model M_j (the reference model is the one with respect to which we compare the observational viability), the posterior probability is given by the following law:

$$\frac{p(M_i|x)}{p(M_j|x)} = \frac{\pi(M_i)}{\pi(M_j)} \frac{p(x|M_i)}{p(x|M_j)} = \frac{\pi(M_i)}{\pi(M_j)} B_{ij}, \quad (16)$$

where the quantity $B_{ij} = \frac{p(x|M_i)}{p(x|M_j)}$ is the Bayes factor of the model M_i with respect to the reference model M_j . Depending on different values of B_{ij} (or equivalently $\ln B_{ij}$) we quantify the observational support of the model M_i over the model M_j . Here we use the widely accepted Jeffreys scales [69] shown in Table II, which imply that for $B_{ij} > 1$ the observational data support model M_i more strongly than model M_j . The negative values of $\ln B_{ij}$ reverse the conclusion, that is the reference model M_j is preferred over M_i .

$\ln B_{ij}$	Strength of evidence for model M_i
$0 \leq \ln B_{ij} < 1$	Weak
$1 \leq \ln B_{ij} < 3$	Definite/Positive
$3 \leq \ln B_{ij} < 5$	Strong
$\ln B_{ij} \geq 5$	Very strong

TABLE II: Revised Jeffreys scale used to quantify the observational support of model M_i with respect to the reference model M_j [69].

In Table III we present the values of $\ln B_{ij}$ calculated for the five one-parameter DE models (9)-(13) analyzed in the previous section, for various observational datasets, compared to the reference Λ CDM scenario. From the values of $\ln B_{ij}$ we can see that Model II and Model III present a better behavior than the other three analyzed models. However, comparing to all models the reference Λ CDM scenario is favored. Nevertheless, we mention here that, interestingly enough, the one-parameter DE parametrizations considered in the present work seem to behave similarly or be less disfavored with respect to Λ CDM scenario comparing with two-parameter DE parametrizations [26, 27, 42, 43]. This is an indication that one-parameter DE models can indeed be efficient in describing the universe evolution.

VI. SUMMARY AND CONCLUSIONS

The phenomenological parametrizations of DE equation of state can be very helpful for the investigation of DE features, since they are of general validity and can describe the DE sector independently of whether it is an extra peculiar fluid in the framework of general relativity or it is effectively of gravitational origin. However, although in the literature there has been a large amount of research on DE parametrizations which involve two or more free parameters, the one-parameter parametrizations seem to be underestimated.

In this work we performed a detailed observational confrontation of several one-parameter DE parametrizations, with various combination datasets. In particular, we used data from cosmic microwave background (CMB) observations, from Joint light-curve analysis sample from Supernovae Type Ia observations (JLA), from baryon acoustic oscillations (BAO) distance measurements, as well as from cosmic chronometers Hubble parameter measurements (CC), and we additionally performed various combined analyses.

Our analyses revealed that all the examined one-parameter dynamical DE models favor a phantom DE equation-of-state at present time w_0 , and this remains valid at more than 95% CL, confirming the result obtained in various other works in different contexts [34, 36, 70, 71, 72, 73, 74, 75, 76]. The inclusion of any external dataset to CMB improves the fitting and decreases the errors significantly without any change in the conclusion. Concerning the present value of the Hubble parameter H_0 , we found that the CMB data alone leads to large error bars, however the inclusion of other datasets decreases them significantly, with the favored H_0 value being in perfect agreement with its direct measurements. Hence, we deduce that one-parameter DE models can provide a solution to the known

Dataset	Model	$\ln B_{ij}$	Strength of evidence for reference Λ CDM scenario
CMB	Model I	-1.9	Definite/Positive
CMB+BAO	Model I	-2.9	Definite/Positive
CMB+BAO+JLA	Model I	-6.0	Very Strong
CMB+BAO+JLA+CC	Model I	-5.2	Very Strong
CMB	Model II	-1.7	Definite/Positive
CMB+BAO	Model II	-2.3	Definite/Positive
CMB+BAO+JLA	Model II	-3.1	Strong
CMB+BAO+JLA+CC	Model II	-3.0	Strong
CMB	Model III	-1.6	Definite/Positive
CMB+BAO	Model III	-2.6	Definite/Positive
CMB+BAO+JLA	Model III	-4.2	Strong
CMB+BAO+JLA+CC	Model III	-3.9	Strong
CMB	Model IV	-2.1	Definite/Positive
CMB+BAO	Model IV	-3.7	Strong
CMB+BAO+JLA	Model IV	-6.9	Very Strong
CMB+BAO+JLA+CC	Model IV	-7.2	Very Strong
CMB	Model V	-2.8	Definite/Positive
CMB+BAO	Model V	-2.9	Definite/Positive
CMB+BAO+JLA	Model V	-5.8	Very Strong
CMB+BAO+JLA+CC	Model V	-5.3	Very Strong

TABLE III: Summary of the Bayes factors values $\ln B_{ij}$ calculated for the five one-parameter DE models (9)-(13), with respect to the reference Λ CDM scenario. The negative sign indicates that the reference scenario is preferred over the fitted models.

H_0 -tension between local measurements and Planck indirect ones. This is one of the main results of the present work. Nevertheless, the possible σ_8 -tension does not seem to be reconciled, since in all models the favored σ_8 value is similar to the Planck's estimated one.

Lastly, in order to examine which of the five models is better fitted to the data, as well as in order to compare them with the standard Λ CDM cosmological scenario, we compute their Bayesian evidences using the `MCEvidence` (summarized in Table III). As we saw Model II and Model III are relatively close to Λ CDM (this can also be viewed from the Whisker graph in Fig. 2 where w_0 for Model II and Model III are relatively close to $w_0 = -1$ compared to other models). However, the reference Λ CDM scenario is still favored compared to all one parameter dynamical DE models. Nevertheless, these one-parameter DE models have similar or better efficiency in fitting the data comparing with the two-parameter DE parametrizations analyzed in the literature, taking into account their advantage that they are more economical and have one free parameter less. This is an indication that one-parameter DE models can indeed be efficient in describing the universe evolution, and thus they deserve a thorough investigation.

Acknowledgments

The authors would like to thank an anonymous referee for essential suggestions that improved the presentation and the quality of the manuscript. WY was supported by the National Natural Science Foundation of China under Grants No. 11705079 and No. 11647153. SP acknowledges the research grant under Faculty Research and Professional Development Fund (FRPDF) Scheme of Presidency University, Kolkata, India. EDV acknowledges support from the European Research Council in the form of a Consolidator Grant with number 681431. SC acknowledges the Mathematical Research Impact Centric Support (MATRICS), project reference no. MTR/2017/000407, by the Science and Engineering Research Board, Government of India. This article is based upon work from CANTATA COST (European Cooperation in Science and Technology) action CA15117, EU Framework Programme Horizon 2020.

Parameters	CMB	CMB+BAO	CMB+BAO+JLA	CMB+BAO+JLA+CC
$\Omega_c h^2$	$0.1200^{+0.0015+0.0028}_{-0.0015-0.0029}$	$0.1182^{+0.0014+0.0025}_{-0.0014-0.0027}$	$0.1172^{+0.0012+0.0023}_{-0.0012-0.0023}$	$0.1174^{+0.0012+0.0024}_{-0.0012-0.0023}$
$\Omega_b h^2$	$0.02218^{+0.00016+0.00032}_{-0.00016-0.00031}$	$0.02230^{+0.00014+0.00032}_{-0.00017-0.00030}$	$0.02237^{+0.00015+0.00030}_{-0.00015-0.00030}$	$0.02235^{+0.00015+0.00028}_{-0.00014-0.00029}$
$100\theta_{MC}$	$1.04039^{+0.00033+0.00067}_{-0.00033-0.00063}$	$1.04070^{+0.00035+0.00067}_{-0.00035-0.00067}$	$1.04078^{+0.00030+0.00063}_{-0.00033-0.00057}$	$1.04075^{+0.00030+0.00059}_{-0.00029-0.00061}$
τ	$0.081^{+0.019+0.033}_{-0.017-0.035}$	$0.091^{+0.018+0.033}_{-0.018-0.035}$	$0.098^{+0.017+0.034}_{-0.017-0.033}$	$0.097^{+0.017+0.033}_{-0.017-0.032}$
n_s	$0.9727^{+0.0046+0.0090}_{-0.0046-0.0092}$	$0.9772^{+0.0045+0.0100}_{-0.0054-0.0088}$	$0.9794^{+0.0042+0.0081}_{-0.0040-0.0080}$	$0.9789^{+0.0039+0.0082}_{-0.0041-0.0081}$
$\ln(10^{10} A_s)$	$3.106^{+0.037+0.066}_{-0.033-0.068}$	$3.121^{+0.034+0.070}_{-0.034-0.069}$	$3.133^{+0.032+0.065}_{-0.033-0.065}$	$3.132^{+0.033+0.065}_{-0.032-0.063}$
w_0	$< -1.45 < -1.08$	$-1.48^{+0.11+0.17}_{-0.10-0.17}$	$-1.355^{+0.049+0.084}_{-0.044-0.085}$	$-1.367^{+0.048+0.092}_{-0.044-0.090}$
Ω_{m0}	$0.268^{+0.038+0.13}_{-0.081-0.10}$	$0.271^{+0.014+0.029}_{-0.017-0.027}$	$0.293^{+0.008+0.017}_{-0.008-0.017}$	$0.291^{+0.009+0.018}_{-0.009-0.017}$
σ_8	$0.887^{+0.094+0.13}_{-0.061-0.14}$	$0.864^{+0.029+0.051}_{-0.025-0.054}$	$0.833^{+0.017+0.034}_{-0.019-0.032}$	$0.837^{+0.016+0.036}_{-0.018-0.034}$
H_0	74^{+11+14}_{-7-15}	$72.2^{+2.3+3.9}_{-2.1-3.9}$	$69.2^{+1.1+2.0}_{-1.0-1.9}$	$69.5^{+1.1+2.1}_{-1.1-2.2}$

TABLE IV: Summary of the 68% and 95% CL constraints on Model I of (9), namely $w_x(a) = w_0 \exp(a-1)$, using various combinations of the observational data sets. Ω_{m0} is the current value of $\Omega_m = \Omega_b + \Omega_c$, while H_0 is in units of $\text{km s}^{-1} \text{Mpc}^{-1}$.

Parameters	CMB	CMB+BAO	CMB+BAO+JLA	CMB+BAO+JLA+CC
$\Omega_c h^2$	$0.1198^{+0.0014+0.0031}_{-0.0016-0.0030}$	$0.1191^{+0.0013+0.0025}_{-0.0012-0.0025}$	$0.1187^{+0.0012+0.0024}_{-0.0011-0.0022}$	$0.1186^{+0.0012+0.0023}_{-0.0012-0.0023}$
$\Omega_b h^2$	$0.02220^{+0.00016+0.00031}_{-0.00016-0.00031}$	$0.02224^{+0.00014+0.0003}_{-0.00016-0.00029}$	$0.02226^{+0.00014+0.00026}_{-0.00014-0.00027}$	$0.02227^{+0.00014+0.00029}_{-0.00015-0.00030}$
$100\theta_{MC}$	$1.04042^{+0.00035+0.00068}_{-0.00035-0.00069}$	$1.04054^{+0.00034+0.00058}_{-0.00031-0.00062}$	$1.04057^{+0.00032+0.00059}_{-0.00030-0.00060}$	$1.04062^{+0.00034+0.00059}_{-0.00032-0.00062}$
τ	$0.078^{+0.018+0.035}_{-0.018-0.034}$	$0.088^{+0.019+0.031}_{-0.016-0.034}$	$0.092^{+0.017+0.033}_{-0.017-0.035}$	$0.092^{+0.018+0.034}_{-0.017-0.033}$
n_s	$0.9728^{+0.0046+0.0094}_{-0.0047-0.0090}$	$0.9752^{+0.0042+0.0078}_{-0.0044-0.0078}$	$0.9766^{+0.0041+0.0081}_{-0.0041-0.0082}$	$0.9769^{+0.0043+0.0082}_{-0.0043-0.008}$
$\ln(10^{10} A_s)$	$3.100^{+0.035+0.068}_{-0.035-0.065}$	$3.118^{+0.036+0.060}_{-0.031-0.066}$	$3.125^{+0.033+0.064}_{-0.033-0.068}$	$3.124^{+0.034+0.066}_{-0.035-0.066}$
w_0	$-1.53^{+0.21}_{-0.39} < -1.32$	$-1.196^{+0.057+0.11}_{-0.055-0.11}$	$-1.135^{+0.041+0.074}_{-0.037-0.078}$	$-1.130^{+0.039+0.073}_{-0.038-0.073}$
Ω_{m0}	$0.225^{+0.033+0.120}_{-0.074-0.093}$	$0.284^{+0.011+0.022}_{-0.012-0.022}$	$0.297^{+0.009+0.017}_{-0.009-0.017}$	$0.298^{+0.009+0.017}_{-0.009-0.017}$
σ_8	$0.95^{+0.10+0.14}_{-0.07-0.16}$	$0.853^{+0.020+0.040}_{-0.021-0.040}$	$0.836^{+0.018+0.036}_{-0.018-0.038}$	$0.833^{+0.019+0.034}_{-0.017-0.034}$
H_0	81^{+12+18}_{-9-18}	$70.7^{+1.4+2.9}_{-1.4-2.9}$	$69.0^{+1.0+2.0}_{-1.1-1.9}$	$68.9^{+0.9+1.9}_{-1.1-1.8}$

TABLE V: Summary of the 68% and 95% CL constraints on Model II of (10), namely $w_x(a) = w_0 a[1 - \log(a)]$, using various combinations of the observational data sets. Ω_{m0} is the current value of $\Omega_m = \Omega_b + \Omega_c$, while H_0 is in units of $\text{km s}^{-1} \text{Mpc}^{-1}$.

Appendix: THE TABLES

In this Appendix we present all Tables that display the summary of the 68% and 95% CL constraints, using various datasets, for all the one-parameters models investigated in the main text.

- [1] S. Weinberg, *The Cosmological Constant Problem*, Rev. Mod. Phys. **61**, 1 (1989).
- [2] E. J. Copeland, M. Sami and S. Tsujikawa, *Dynamics of dark energy*, Int. J. Mod. Phys. D **15**, 1753 (2006).
- [3] Y. F. Cai, E. N. Saridakis, M. R. Setare and J. Q. Xia, *Quintom Cosmology: Theoretical implications and observations*, Phys. Rept. **493**, 1 (2010).
- [4] S. Nojiri and S. D. Odintsov, *Introduction to modified gravity and gravitational alternative for dark energy*, eConf C **0602061**, 06 (2006) [Int. J. Geom. Meth. Mod. Phys. **04**, 115 (2007)].
- [5] S. Capozziello and M. De Laurentis, *Extended Theories of Gravity*, Phys. Rept. **509**, 167 (2011).
- [6] Y. F. Cai, S. Capozziello, M. De Laurentis and E. N. Saridakis, *f(T) teleparallel gravity and cosmology*, Rept. Prog. Phys. **79**, no. 10, 106901 (2016).
- [7] M. Chevallier and D. Polarski, *Accelerating universes with scaling dark matter*, Int. J. Mod. Phys. D **10**, 213 (2001).
- [8] E. V. Linder, *Exploring the expansion history of the universe*, Phys. Rev. Lett. **90**, 091301 (2003).
- [9] A. R. Cooray and D. Huterer, *Gravitational lensing as a probe of quintessence*, Astrophys. J. **513**, L95 (1999).

Parameters	CMB	CMB+BAO	CMB+BAO+JLA	CMB+BAO+JLA+CC
$\Omega_c h^2$	$0.1198^{+0.0015+0.0029}_{-0.0015-0.0028}$	$0.1196^{+0.0012+0.0023}_{-0.0012-0.0022}$	$0.1190^{+0.0011+0.0023}_{-0.0012-0.0022}$	$0.1190^{+0.0012+0.0024}_{-0.0013-0.0024}$
$\Omega_b h^2$	$0.02220^{+0.00016+0.00031}_{-0.00015-0.00031}$	$0.02221^{+0.00014+0.00027}_{-0.00014-0.00026}$	$0.02223^{+0.00014+0.00027}_{-0.00015-0.00029}$	$0.02223^{+0.00015+0.00030}_{-0.00015-0.00029}$
$100\theta_{MC}$	$1.04044^{+0.00034+0.00069}_{-0.00033-0.00068}$	$1.04045^{+0.00029+0.00060}_{-0.00030-0.00058}$	$1.04052^{+0.00030+0.00061}_{-0.00033-0.00061}$	$1.04052^{+0.00030+0.00060}_{-0.00030-0.00064}$
τ	$0.078^{+0.017+0.032}_{-0.017-0.034}$	$0.089^{+0.017+0.032}_{-0.017-0.033}$	$0.094^{+0.017+0.033}_{-0.017-0.033}$	$0.095^{+0.018+0.033}_{-0.018-0.035}$
n_s	$0.9733^{+0.0046+0.0088}_{-0.0045-0.0088}$	$0.9748^{+0.0040+0.0073}_{-0.0038-0.0077}$	$0.9767^{+0.0044+0.0086}_{-0.0044-0.0084}$	$0.9765^{+0.0042+0.0088}_{-0.0044-0.0083}$
$\ln(10^{10} A_s)$	$3.100^{+0.035+0.064}_{-0.032-0.066}$	$3.119^{+0.034+0.064}_{-0.033-0.066}$	$3.128^{+0.033+0.065}_{-0.033-0.067}$	$3.129^{+0.035+0.065}_{-0.034-0.068}$
w_0	$-1.63^{+0.16}_{-0.33} < -1.25$	$-1.239^{+0.060+0.096}_{-0.049-0.11}$	$-1.162^{+0.038+0.074}_{-0.037-0.072}$	$-1.163^{+0.041+0.071}_{-0.035-0.077}$
Ω_{m0}	$0.207^{+0.028+0.086}_{-0.056-0.070}$	$0.279^{+0.011+0.023}_{-0.012-0.021}$	$0.295^{+0.009+0.017}_{-0.010-0.017}$	$0.295^{+0.008+0.016}_{-0.008-0.016}$
σ_8	$0.969^{+0.085+0.12}_{-0.059-0.13}$	$0.857^{+0.020+0.042}_{-0.021-0.042}$	$0.832^{+0.017+0.037}_{-0.017-0.036}$	$0.833^{+0.018+0.033}_{-0.018-0.034}$
H_0	$84.^{+10+15}_{-8-15}$	$71.4^{+1.4+3.0}_{-1.6-2.8}$	$69.4^{+1.0+2.0}_{-1.0-1.9}$	$69.4^{+0.9+1.9}_{-1.0-1.8}$

TABLE VI: Summary of the 68% and 95% CL constraints on Model III of (11), namely $w_x(a) = w_0 a \exp(1-a)$, using various combinations of the observational data sets. Ω_{m0} is the current value of $\Omega_m = \Omega_b + \Omega_c$, while H_0 is in units of $\text{km s}^{-1} \text{Mpc}^{-1}$.

Parameters	CMB	CMB+BAO	CMB+BAO+JLA	CMB+BAO+JLA+CC
$\Omega_c h^2$	$0.1201^{+0.0015+0.0031}_{-0.0015-0.0029}$	$0.1199^{+0.0012+0.0022}_{-0.0012-0.0022}$	$0.1196^{+0.0011+0.0022}_{-0.0011-0.0022}$	$0.1194^{+0.0010+0.0021}_{-0.0011-0.0021}$
$\Omega_b h^2$	$0.02217^{+0.00017+0.00030}_{-0.00015-0.00031}$	$0.02217^{+0.00015+0.00029}_{-0.00015-0.00029}$	$0.02218^{+0.00014+0.00026}_{-0.00014-0.00029}$	$0.02220^{+0.00015+0.00028}_{-0.00014-0.00028}$
$100\theta_{MC}$	$1.04038^{+0.00033+0.00067}_{-0.00033-0.00066}$	$1.04038^{+0.00030+0.00058}_{-0.00030-0.00056}$	$1.04042^{+0.00032+0.00057}_{-0.00028-0.00062}$	$1.04044^{+0.00030+0.00062}_{-0.00033-0.00059}$
τ	$0.080^{+0.017+0.034}_{-0.018-0.033}$	$0.091^{+0.017+0.035}_{-0.017-0.034}$	$0.098^{+0.017+0.032}_{-0.017-0.031}$	$0.099^{+0.019+0.033}_{-0.017-0.035}$
n_s	$0.9728^{+0.0043+0.0086}_{-0.0043-0.0088}$	$0.9747^{+0.0040+0.0078}_{-0.0041-0.0079}$	$0.9765^{+0.0041+0.0077}_{-0.0040-0.0081}$	$0.9769^{+0.0041+0.0079}_{-0.0040-0.0078}$
$\ln(10^{10} A_s)$	$3.104^{+0.032+0.066}_{-0.033-0.064}$	$3.125^{+0.033+0.070}_{-0.033-0.067}$	$3.136^{+0.033+0.062}_{-0.033-0.061}$	$3.137^{+0.037+0.065}_{-0.034-0.068}$
w_0	$< -1.58 < -1.34$	$-1.353^{+0.065+0.12}_{-0.056-0.12}$	$-1.248^{+0.036+0.069}_{-0.033-0.071}$	$-1.244^{+0.034+0.077}_{-0.036-0.076}$
Ω_{m0}	$0.206^{+0.025+0.080}_{-0.052-0.062}$	$0.268^{+0.012+0.024}_{-0.012-0.023}$	$0.290^{+0.008+0.016}_{-0.008-0.016}$	$0.290^{+0.008+0.018}_{-0.010-0.018}$
σ_8	$0.966^{+0.084+0.11}_{-0.050-0.12}$	$0.865^{+0.021+0.043}_{-0.021-0.043}$	$0.832^{+0.018+0.036}_{-0.018-0.034}$	$0.830^{+0.019+0.035}_{-0.018-0.036}$
H_0	$84.3^{+9.9+13}_{-6.5-14}$	$73.1^{+1.6+3.3}_{-1.8-3.1}$	$70.07^{+0.91+1.9}_{-0.94-1.9}$	$70.04^{+1.01+2.1}_{-0.97-2.1}$

TABLE VII: Summary of the 68% and 95% CL constraints on Model IV of (12), namely $w_x(a) = w_0 a [1 + \sin(1-a)]$, using various combinations of the observational data sets. Ω_{m0} is the current value of $\Omega_m = \Omega_b + \Omega_c$, while H_0 is in units of $\text{km s}^{-1} \text{Mpc}^{-1}$.

- [10] G. Efstathiou, *Constraining the equation of state of the universe from distant type Ia supernovae and cosmic microwave background anisotropies*, Mon. Not. Roy. Astron. Soc. **310**, 842 (1999).
- [11] P. Astier, *Can luminosity distance measurements probe the equation of state of dark energy*, Phys. Lett. B **500**, 8 (2001).
- [12] J. Weller and A. Albrecht, *Future supernovae observations as a probe of dark energy*, Phys. Rev. D **65**, 103512 (2002).
- [13] H. K. Jassal, J. S. Bagla and T. Padmanabhan, *Observational constraints on low redshift evolution of dark energy: How consistent are different observations?*, Phys. Rev. D **72**, 103503 (2005).
- [14] E. V. Linder and D. Huterer, *How many dark energy parameters?*, Phys. Rev. D **72**, 043509 (2005).
- [15] Y. g. Gong and Y. Z. Zhang, *Probing the curvature and dark energy*, Phys. Rev. D **72**, 043518 (2005).
- [16] S. Nesseris and L. Perivolaropoulos, *Comparison of the legacy and gold snia dataset constraints on dark energy models*, Phys. Rev. D **72**, 123519 (2005).
- [17] B. Feng, M. Li, Y. S. Piao and X. Zhang, *Oscillating quintom and the recurrent universe*, Phys. Lett. B **634**, 101 (2006).
- [18] J. Q. Xia, G. B. Zhao, H. Li, B. Feng and X. Zhang, *Features in Dark Energy Equation of State and Modulations in the Hubble Diagram*, Phys. Rev. D **74**, 083521 (2006).
- [19] S. Basilakos and N. Voglis, *Virialization of cosmological structures in models with time varying equation of state*, Mon. Not. Roy. Astron. Soc. **374**, 269 (2007).
- [20] S. Nojiri and S. D. Odintsov, *The Oscillating dark energy: Future singularity and coincidence problem*, Phys. Lett. B **637**, 139 (2006).
- [21] E. N. Saridakis, *Theoretical Limits on the Equation-of-State Parameter of Phantom Cosmology*, Phys. Lett. B **676**, 7 (2009).
- [22] E. M. Barboza, Jr. and J. S. Alcaniz, *A parametric model for dark energy*, Phys. Lett. B **666**, 415 (2008).

Parameters	CMB	CMB+BAO	CMB+BAO+JLA	CMB+BAO+JLA+CC
$\Omega_c h^2$	$0.1201^{+0.0016+0.0033}_{-0.0016-0.0033}$	$0.1196^{+0.0012+0.0023}_{-0.0011-0.0023}$	$0.1191^{+0.0012+0.0023}_{-0.0012-0.0024}$	$0.1191^{+0.0011+0.0024}_{-0.0013-0.0023}$
$\Omega_b h^2$	$0.02217^{+0.00017+0.00034}_{-0.00017-0.00034}$	$0.02219^{+0.00014+0.00027}_{-0.00014-0.00029}$	$0.02223^{+0.00014+0.00027}_{-0.00014-0.00029}$	$0.02223^{+0.00014+0.00028}_{-0.00014-0.00027}$
$100\theta_{MC}$	$1.04037^{+0.00035+0.00067}_{-0.00034-0.00069}$	$1.04042^{+0.00029+0.00060}_{-0.00030-0.00058}$	$1.04046763^{+0.00034+0.00058}_{-0.00028-0.00062}$	$1.04053^{+0.00031+0.00060}_{-0.00031-0.00059}$
τ	$0.079^{+0.018+0.035}_{-0.018-0.035}$	$0.092^{+0.018+0.035}_{-0.017-0.036}$	$0.099^{+0.017+0.037}_{-0.017-0.037}$	$0.097^{+0.017+0.034}_{-0.017-0.034}$
n_s	$0.9727^{+0.0045+0.0090}_{-0.0046-0.0091}$	$0.9749^{+0.0041+0.0086}_{-0.0042-0.0080}$	$0.9772^{+0.0040+0.0087}_{-0.0046-0.0081}$	$0.9766^{+0.0040+0.0080}_{-0.0040-0.0079}$
$\ln(10^{10} A_s)$	$3.103^{+0.035+0.067}_{-0.035-0.068}$	$3.125^{+0.035+0.065}_{-0.034-0.070}$	$3.136^{+0.033+0.065}_{-0.033-0.073}$	$3.134^{+0.033+0.065}_{-0.033-0.065}$
w_0	$< -1.52 < -1.20$	$-1.308^{+0.063+0.12}_{-0.074-0.12}$	$-1.213^{+0.045+0.074}_{-0.037-0.086}$	$-1.213^{+0.033+0.062}_{-0.032-0.062}$
Ω_{m0}	$0.215^{+0.027+0.105}_{-0.064-0.080}$	$0.273^{+0.012+0.027}_{-0.015-0.025}$	$0.293^{+0.009+0.018}_{-0.009-0.019}$	$0.293^{+0.008+0.017}_{-0.009-0.017}$
σ_8	$0.955^{+0.094+0.13}_{-0.059-0.15}$	$0.861^{+0.023+0.048}_{-0.025-0.045}$	$0.831^{+0.017+0.038}_{-0.017-0.035}$	$0.830^{+0.016+0.035}_{-0.016-0.033}$
H_0	$82.9^{+12+15}_{-7.0-17}$	$72.3^{+2.0+3.3}_{-1.7-3.4}$	$69.6^{+1.0+2.3}_{-1.2-2.0}$	$69.64^{+0.92+1.9}_{-0.94-1.8}$

TABLE VIII: Summary of the 68% and 95% CL constraints on Model V of (13), namely $w_x(a) = w_0 a[1 + \arcsin(1 - a)]$, using various combinations of the observational data sets. Here, Ω_{m0} is the current value of $\Omega_m = \Omega_b + \Omega_c$, while H_0 is in units of $\text{km s}^{-1} \text{Mpc}^{-1}$.

- [23] E. N. Saridakis, *Phantom evolution in power-law potentials*, Nucl. Phys. B **819**, 116 (2009).
- [24] S. Dutta, E. N. Saridakis and R. J. Scherrer, *Dark energy from a quintessence (phantom) field rolling near potential minimum (maximum)*, Phys. Rev. D **79**, 103005 (2009).
- [25] E. N. Saridakis, *Quintom evolution in power-law potentials*, Nucl. Phys. B **830**, 374 (2010).
- [26] J. Z. Ma and X. Zhang, *Probing the dynamics of dark energy with novel parametrizations*, Phys. Lett. B **699**, 233 (2011).
- [27] L. Feng and T. Lu, *A new equation of state for dark energy model*, JCAP **1111**, 034 (2011).
- [28] C. J. Feng, X. Y. Shen, P. Li and X. Z. Li, *A New Class of Parametrization for Dark Energy without Divergence*, JCAP **1209**, 023 (2012).
- [29] A. De Felice, S. Nesseris and S. Tsujikawa, *Observational constraints on dark energy with a fast varying equation of state*, JCAP **1205**, 029 (2012).
- [30] X. m. Chen, Y. Gong, E. N. Saridakis and Y. Gong, *Time-dependent interacting dark energy and transient acceleration*, Int. J. Theor. Phys. **53**, 469 (2014).
- [31] S. Basilakos and J. Solá, *Effective equation of state for running vacuum: mirage quintessence and phantom dark energy*, Mon. Not. Roy. Astron. Soc. **437**, no. 4, 3331 (2014).
- [32] C. Umiltà, M. Ballardini, F. Finelli and D. Paoletti, *CMB and BAO constraints for an induced gravity dark energy model with a quartic potential*, JCAP **1508**, 017 (2015).
- [33] M. Ballardini, F. Finelli, C. Umilt and D. Paoletti, *Cosmological constraints on induced gravity dark energy models*, JCAP **1605**, no. 05, 067 (2016).
- [34] E. Di Valentino, A. Melchiorri and J. Silk, *Reconciling Planck with the local value of H_0 in extended parameter space*, Phys. Lett. B **761**, 242 (2016).
- [35] R. Chávez, M. Plionis, S. Basilakos, R. Terlevich, E. Terlevich, J. Melnick, F. Bresolin and A. L. González-Morán, *Constraining the dark energy equation of state with HII galaxies*, Mon. Not. Roy. Astron. Soc. **462**, no. 3, 2431 (2016).
- [36] E. Di Valentino, A. Melchiorri, E. V. Linder and J. Silk, *Constraining Dark Energy Dynamics in Extended Parameter Space*, Phys. Rev. D **96**, 023523 (2017).
- [37] E. Di Valentino, *Crack in the cosmological paradigm*, Nat. Astron. **1**, 569 (2017).
- [38] G. B. Zhao *et al.*, *Dynamical dark energy in light of the latest observations*, Nat. Astron. **1**, 627 (2017).
- [39] E. Di Valentino, E. V. Linder and A. Melchiorri, *Vacuum phase transition solves the H_0 tension*, Phys. Rev. D **97**, no. 4, 043528 (2018).
- [40] W. Yang, R. C. Nunes, S. Pan and D. F. Mota, *Effects of neutrino mass hierarchies on dynamical dark energy models*, Phys. Rev. D **95**, 103522 (2017).
- [41] R. J. F. Marcondes and S. Pan, *Cosmic chronometers constraints on some fast-varying dark energy equations of state* [arXiv:1711.06157 [astro-ph.CO]].
- [42] W. Yang, S. Pan and A. Paliathanasis, *Latest astronomical constraints on some nonlinear parametric dark energy models*, Mon. Not. Roy. Astron. Soc. **475**, 2605 (2018).
- [43] S. Pan, E. N. Saridakis and W. Yang, *Observational Constraints on Oscillating Dark-Energy Parametrizations*, Phys. Rev. D **98**, no. 6, 063510 (2018).
- [44] S. Vagnozzi, S. Dhawan, M. Gerbino, K. Freese, A. Goobar and O. Mena, *Constraints on the sum of the neutrino masses in dynamical dark energy models with $w(z) \geq -1$ are tighter than those obtained in Λ CDM*, Phys. Rev. D **98**, no. 8, 083501 (2018).
- [45] V. F. Mukhanov, H. A. Feldman and R. H. Brandenberger, *Theory of cosmological perturbations*, Phys. Rept. **215**, 203 (1992).

- [46] C. P. Ma and E. Bertschinger, *Cosmological perturbation theory in the synchronous and conformal Newtonian gauges*, *Astrophys. J.* **455**, 7 (1995).
- [47] K. A. Malik and D. Wands, *Cosmological perturbations*, *Phys. Rept.* **475**, 1 (2009).
- [48] R. Adam *et al.* [Planck Collaboration], *Planck 2015 results. I. Overview of products and scientific results*, *Astron. Astrophys.* **594**, A1 (2016).
- [49] N. Aghanim *et al.* [Planck Collaboration], *Planck 2015 results. XI. CMB power spectra, likelihoods, and robustness of parameters*, *Astron. Astrophys.* **594**, A11 (2016).
- [50] M. Betoule *et al.* [SDSS Collaboration], *Improved cosmological constraints from a joint analysis of the SDSS-II and SNLS supernova samples*, *Astron. Astrophys.* **568**, A22 (2014).
- [51] F. Beutler *et al.*, *The 6dF Galaxy Survey: Baryon Acoustic Oscillations and the Local Hubble Constant*, *Mon. Not. Roy. Astron. Soc.* **416**, 3017 (2011).
- [52] A. J. Ross, L. Samushia, C. Howlett, W. J. Percival, A. Burden and M. Manera, *The clustering of the SDSS DR7 main Galaxy sample I. A 4 per cent distance measure at $z = 0.15$* , *Mon. Not. Roy. Astron. Soc.* **449**, no. 1, 835 (2015).
- [53] H. Gil-Marín *et al.*, *The clustering of galaxies in the SDSS-III Baryon Oscillation Spectroscopic Survey: BAO measurement from the LOS-dependent power spectrum of DR12 BOSS galaxies*, *Mon. Not. Roy. Astron. Soc.* **460**, no. 4, 4210 (2016).
- [54] M. Moresco *et al.*, *A 6% measurement of the Hubble parameter at $z \sim 0.45$: direct evidence of the epoch of cosmic re-acceleration*, *JCAP* **1605**, no. 05, 014 (2016).
- [55] A. Lewis and S. Bridle, *Cosmological parameters from CMB and other data: A Monte Carlo approach*, *Phys. Rev. D* **66**, 103511 (2002).
- [56] A. Lewis, *Efficient sampling of fast and slow cosmological parameters*, *Phys. Rev. D* **87**, no. 10, 103529 (2013).
- [57] A. G. Riess *et al.*, *“A 2.4% Determination of the Local Value of the Hubble Constant,”* *Astrophys. J.* **826**, 56 (2016).
- [58] A. G. Riess *et al.*, *New Parallaxes of Galactic Cepheids from Spatially Scanning the Hubble Space Telescope: Implications for the Hubble Constant*, *Astrophys. J.* **855**, 136 (2018).
- [59] S. Birrer *et al.*, *H0LiCOW - IX. Cosmographic analysis of the doubly imaged quasar SDSS 1206+4332 and a new measurement of the Hubble constant*, arXiv:1809.01274 [astro-ph.CO].
- [60] C. Heymans *et al.*, *CFHTLenS: The Canada-France-Hawaii Telescope Lensing Survey*, *Mon. Not. Roy. Astron. Soc.* **427**, 146 (2012).
- [61] T. Erben *et al.*, *CFHTLenS: The Canada-France-Hawaii Telescope Lensing Survey - Imaging Data and Catalogue Products*, *Mon. Not. Roy. Astron. Soc.* **433**, 2545 (2013).
- [62] H. Hildebrandt *et al.*, *KiDS-450: Cosmological parameter constraints from tomographic weak gravitational lensing*, *Mon. Not. Roy. Astron. Soc.* **465**, 1454 (2017).
- [63] T. M. C. Abbott *et al.* [DES Collaboration], *Dark Energy Survey Year 1 Results: Cosmological Constraints from Galaxy Clustering and Weak Lensing*, *Phys. Rev. D* **98**, no. 4, 043526 (2018).
- [64] N. Aghanim *et al.* [Planck Collaboration], *Planck 2018 results. VI. Cosmological parameters*, arXiv:1807.06209 [astro-ph.CO].
- [65] W. Lin and M. Ishak, *Cosmological discordances II: Hubble constant, Planck and large-scale-structure data sets*, *Phys. Rev. D* **96**, no. 8, 083532 (2017).
- [66] P. A. R. Ade *et al.* [Planck Collaboration], *Planck 2015 results. XIII. Cosmological parameters*, *Astron. Astrophys.* **594**, A13 (2016).
- [67] A. Heavens, Y. Fantaye, A. Mootoivaloo, H. Eggers, Z. Hosenie, S. Kroon and E. Sellentin, *Marginal Likelihoods from Monte Carlo Markov Chains*, arXiv:1704.03472 [stat.CO].
- [68] A. Heavens, Y. Fantaye, E. Sellentin, H. Eggers, Z. Hosenie, S. Kroon and A. Mootoivaloo, *No evidence for extensions to the standard cosmological model*, *Phys. Rev. Lett.* **119**, no. 10, 101301 (2017).
- [69] R. E. Kass and A. E. Raftery, *Bayes factors*, *J. Am. Statist. Assoc.* **90**, no.430, 773 (1995).
- [70] E. Di Valentino, A. Melchiorri and O. Mena, *Can interacting dark energy solve the H_0 tension?*, *Phys. Rev. D* **96**, no. 4, 043503 (2017).
- [71] E. Di Valentino, A. Melchiorri and J. Silk, *Beyond six parameters: extending Λ CDM*, *Phys. Rev. D* **92**, no.12, 121302 (2015).
- [72] W. Yang, S. Pan and D. F. Mota, *Novel approach toward the large-scale stable interacting dark-energy models and their astronomical bounds*, *Phys. Rev. D* **96**, no. 12, 123508 (2017).
- [73] W. Yang, S. Pan and J. D. Barrow, *Large-scale Stability and Astronomical Constraints for Coupled Dark-Energy Models*, *Phys. Rev. D* **97**, no. 4, 043529 (2018).
- [74] E. Mörtzell and S. Dhawan, *Does the Hubble constant tension call for new physics?*, *JCAP* **1809**, no.09, 025 (2018).
- [75] W. Yang, S. Pan, E. Di Valentino, R. C. Nunes, S. Vagnozzi and D. F. Mota, *Tale of stable interacting dark energy, observational signatures, and the H_0 tension,*, *JCAP* **1809**, no. 09, 019, (2018).
- [76] W. Yang, A. Mukherjee, E. Di Valentino and S. Pan, *Interacting dark energy with time varying equation of state and the H_0 tension*, *Phys. Rev. D* **98**, no. 12, 123527 (2018).